Supporting Information

Inose et al. 10.1073/pnas.0909311106

SI Text

Cell Culture. C2C12 cells and MC3T3-E1 cells were maintained under standard conditions. Osteogenic differentiation of C2C12 cells was induced by adding 50 or 100 ng/mL BMP-2. Primary osteoblast cultures were established as described in ref. 1. Briefly, we isolated primary osteoblasts from calvariae of 4-day-old mice using Trypsin EDTA (Gibco) and Collagenase P (Sigma) and cultured them in α-MEM (Sigma) containing ascorbic acid (0.1 mg/mL; Sigma) and β-glycerophosphate (5 mM). We performed all the cell cultures in triplicate or quadruplicate wells and repeated experiments more than four times. For the establishment of stable cell lines, we constructed lentivirus-expressing miR-206 using the vira power lentiviral gateway system (Invitrogen), as described by the manufacturer. Stable clones expressing miR-206 or lacZ were selected by 5 μg/mL blasticidin (Invitrogen).

Microarrays. C2C12 cells were induced to osteoblasts or maintained in growth medium. Total RNA from each sample was isolated on day 2 using TRIzol. Small RNAs containing miRNAs were isolated from total RNA using the mirVana miRNA isolation kit (Ambion) according to the manufacturer's instructions. Microarray analysis was performed as described in ref. 2.

Cloning and Gene Expression. Genomic fragments of miR-206 precursors were amplified by PCR using mouse genomic DNA. The PCR products were cloned into the pcDNA3.1 vector (Invitrogen) or the pAd/CMV/V5 vector (Invitrogen) to generate adenoviral vectors. For adenoviral expression, cells were infected with 100 plaque-forming U/cell of adenovirus. For knockdown of miR-206, 50 nM miRIDIAN microRNA Inhibitor (Dharmacon) was transfected with HiPerFect reagent (Qiagen). miRNA expression was detected by an RNase protection assay using a mirVANA mRNA probe construction and detection kit (Ambion) or quantitative RT-PCR with Mx3000P (Stratagene). TaqMan microRNA assays (Applied Biosystems) were used to quantify the expression of mature miR-206. Gene expression was calculated relative to U6 RNA for miR-206 expression. We used *GAPDH* expression as an internal control for the analysis of the *Akp2*, *Bglap*, *Runx2*, *Osx*, *MyoD*, and *Myf5* genes. Primer sequences are available upon request.

Dual-Luciferase Reporter Assay. For construction of the Cx43–3′-UTR reporter, the CMV promoter was subcloned into the promoterless pGL3-Basic (Promega) upstream of the luciferase gene. We amplified the predicted miR-206 binding sites of the 3′ UTRs of mouse Cx43 by PCR. Then we cloned them into the modified pGL3-basic vector resulting in the Cx43–3′-UTR construct. The activities of firefly luciferase and renilla luciferase in the control vector were determined by the dual-luciferase reporter assay (Promega).

Western Blot Analysis and Immunohistochemistry. Proteins were analyzed by SDS/PAGE, and Western blotting and immunohistochemistry were performed according to a standard protocol (1). For immunohistochemistry, six mice per group were analyzed, and identical results were observed. The antibodies were anti-Connexin 43 (Sigma), anti-GAPDH and anti-BMPR1A (Abcam), anti-Troponin I (Santa Cruz), anti-phospho-Smad1/5 (Cell Signaling). Proteins were detected using ECL advance Western Blotting Detection kit (Amersham Biosciences). Results are representative of more than four individual experiments.

Northern Blot and RNase Protection Assay. Northern blot analysis was performed essentially as reported in ref. 3. The RNase protection assay was performed using the mirVANA mRNA probe construction kit and detection kit (Ambion) according to the manufacturer's instructions.

In Situ Hybridization. microRNA-in situ hybridization was performed as reported in ref. 4 with modifications. Tissue was placed into 4% paraformaldehyde, and fixed for 24 h at 4 °C. Tissue was then placed in 30% sucrose overnight, again at 4 °C. 5′-Digoxigenin (DIG) labeled, LNA-modified oligonucleotide ISH probes were purchased from Exiqon for miR-206, and miR-scramble as background control.

In situ hybridization was performed using DIG labeled riboprobe (α1(I) collagen) and ^{35}S-labeled riboprobe (Runx2) according to the standard protocol as described in ref. 1. Hybridizations were performed at 55 °C.

Double Staining for in Situ Hybridization and Immunohistochemistry. Double staining for in situ hybridization and immunohistochemistry was performed as reported in ref. 4 with modifications. 5′-Digoxigenin (DIG) labeled, LNA-modified oligonucleotide ISH probe for miR-206 (Exiqon), anti-Runx2 (kind gift from Dr. Gerard Karsenty, Columbia University, NY) were used. They were visualized by Alexa Fluor 488 conjugated goat anti-rabbit secondary antibody (Molecular Probes) and TSA Plus Cyanine3 system (Perkin-Elmer). Images were taken with a LSM 510 confocal laser microscope (Zeiss). All images were obtained by restricting the width of emission wavelength by using a spectral slit.

Transgenic Mice. The genomic fragment of the miR-206 precursor was cloned into the PJ-251 plasmid containing a 2.3-kb α1(I) collagen promoter and a poly (A) site (5). Inserts were microinjected into C57BL/6 mouse embryos and implanted into pseudopregnant foster female mice as described in ref. 5. Founder mice were identified by PCR.

All animal experiments were performed with the approval of the Animal Study Committee of Tokyo Medical and Dental University and conformed to relevant guidelines and laws.

Histology and Histomorphometry. We injected calcein (25 mg/kg, Sigma) i.p. 5 and 2 days before sacrifice. We stained undercalcified sections of the third and fourth lumbar vertebrae with von Kossa staining. We performed static and dynamic histomorphometric analysis using the Osteomeasure Analysis System (Osteometrics) as described in ref. 1. We analyzed 8–10 mice for each group.

1. Sato S, et al. (2007) Central control of bone remodeling by neuromedin U. *Nat Med* 13:1234–1240.
2. Hohjoh H, Fukushima T (2007) Marked change in microRNA expression during neuronal differentiation of human teratocarcinoma NTera2D1 and mouse embryonal carcinoma P19 cells. *Biochem Biophys Res Commun* 362:360–367.
3. Saito K, et al. (2006) Specific association of Piwi with rasiRNAs derived from retrotransposon and heterochromatic regions in the Drosophila genome. *Genes Dev* 20:2214–2222.
4. Obernosterer G, Martinez J, Alenius M (2007) Locked nucleic acid-based *in situ* detection of microRNAs in mouse tissue sections. *Nat Protoc* 2:1508–1514.

5. Dacquin R, Starbuck M, Schinke T, Karsenty G (2002) Mouse alpha1(I)-collagen promoter is the best known promoter to drive efficient Cre recombinase expression in osteoblast. *Dev Dyn* 224:245–251.

6. Care A, et al. (2007) MicroRNA-133 controls cardiac hypertrophy. *Nat Med* 13:613–618.

		Genopal	MICM ver2.0	MICM ver2.0
		Sample ID	MR006	MR006
		Sample Name	C2C12Con	C2C12D3
		Normalization Factor	1	0.616219844
miRNA ID	Sequence	Cross hybridization Group	C2C12Con_Signal	C2C12D3_Signal
mmu-miR-1	MIMAT0000123	-		
mmu-miR-7	MIMAT0000677	-		
mmu-miR-9	MIMAT0000142	-		
mmu-miR-10b	MIMAT0000208	-		
mmu-miR-17-3p	MIMAT0000650	-		
mmu-miR-18	MIMAT0000528	-		
mmu-miR-21	MIMAT0000530	-		
mmu-miR-22	MIMAT0000531	-		
mmu-miR-24	MIMAT0000219	-		
mmu-miR-30a-3p	MIMAT0000129	miR-30a-3p		
mmu-miR-31	MIMAT0000538	-		
mmu-miR-32	MIMAT0000654	-		
mmu-miR-96	MIMAT0000541	-		
mmu-miR-103	MIMAT0000546	-		
mmu-miR-122a	MIMAT0000246	-		
mmu-miR-124a	MIMAT0000134	-		
mmu-miR-126-3p	MIMAT0000138	-		
mmu-miR-127	MIMAT0000139	-		
mmu-miR-128a	MIMAT0000140	-		
mmu-miR-129-5p	MIMAT0000209	-		
mmu-miR-132	MIMAT0000144	-		
mmu-miR-133a	MIMAT0000145	-		
mmu-miR-134	MIMAT0000146	-		
mmu-miR-135a	MIMAT0000147	-		
mmu-miR-136	MIMAT0000148	-		
mmu-miR-137	MIMAT0000149	-		
mmu-miR-138	MIMAT0000150	-		
mmu-miR-139	MIMAT0000656	-		
mmu-miR-140	MIMAT0000151	-		
mmu-miR-142-3p	MIMAT0000155	-		
mmu-miR-142-5p	MIMAT0000154	-		
mmu-miR-143	MIMAT0000247	-		
mmu-miR-144	MIMAT0000156	-		
mmu-miR-145	MIMAT0000157	-		
mmu-miR-146	MIMAT0000158	-		
mmu-miR-149	MIMAT0000159	-		
mmu-miR-150	MIMAT0000160	-		
mmu-miR-151	MIMAT0000161	-		
mmu-miR-152	MIMAT0000162	-		
mmu-miR-153	MIMAT0000163	-		
mmu-miR-154	MIMAT0000164	-		
mmu-miR-155	MIMAT0000165	-		
mmu-miR-182	MIMAT0000211	miR-182		
mmu-miR-183	MIMAT0000212	miR-182		
mmu-miR-184	MIMAT0000213	-		
mmu-miR-185	MIMAT0000214	-		
mmu-miR-186	MIMAT0000215	-		
mmu-miR-187	MIMAT0000216	-		
mmu-miR-188	MIMAT0000217	-		
mmu-miR-190	MIMAT0000220	-		
mmu-miR-191	MIMAT0000221	-		
mmu-miR-192	MIMAT0000517	-		
mmu-miR-193	MIMAT0000223	-		
mmu-miR-194	MIMAT0000224	-		

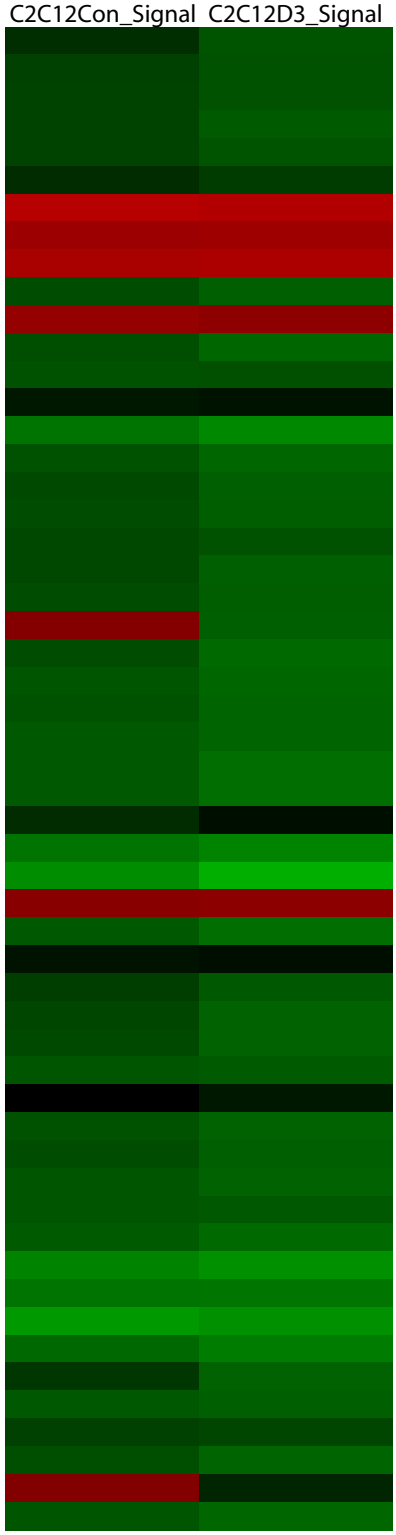

Fig. S1. miRNA array expression data from C2C12 cells cultured in growth medium (Control) or in differentiation medium containing BMP-2. Red denotes high expression and green denotes low expression relative to the median.

mmu-miR-196a	MIMAT0000518	–
mmu-miR-199a	MIMAT0000229	–
mmu-miR-201	MIMAT0000234	–
mmu-miR-202	MIMAT0000235	–
mmu-miR-203	MIMAT0000236	–
mmu-miR-204	MIMAT0000237	–
mmu-miR-205	MIMAT0000238	–
mmu-miR-206	MIMAT0000239	–
mmu-miR-207	MIMAT0000240	–
mmu-miR-208	MIMAT0000520	–
mmu-miR-210	MIMAT0000658	–
mmu-miR-213	MIMAT0000660	–
mmu-miR-291-5p	MIMAT0000367	–
mmu-miR-292-3p	MIMAT0000370	–
mmu-miR-293	MIMAT0000371	–
mmu-miR-295	MIMAT0000373	–
mmu-miR-296	MIMAT0000374	–
mmu-miR-297	MIMAT0000375	–
mmu-miR-298	MIMAT0000376	–
mmu-miR-299	MIMAT0000377	–
mmu-miR-301	MIMAT0000379	–
mmu-miR-302	MIMAT0000380	–
mmu-miR-324-3p	MIMAT0000556	–
mmu-miR-324-5p	MIMAT0000555	–
mmu-miR-328	MIMAT0000565	–
mmu-miR-337	MIMAT0000578	–
mmu-miR-344	MIMAT0000593	–
mmu-miR-350	MIMAT0000605	–
mmu-miR-361	MIMAT0000704	–
mmu-miR-370	MIMAT0001095	–
mmu-miR-375	MIMAT0000739	–
mmu-miR-376a	MIMAT0000740	–
mmu-miR-376b	MIMAT0001092	–
mmu-miR-377	MIMAT0000741	–
mmu-miR-378	MIMAT0000742	–
mmu-miR-379	MIMAT0000743	–
mmu-miR-380-3p	MIMAT0000745	–
mmu-miR-380-5p	MIMAT0000744	–
mmu-miR-382	MIMAT0000747	–
mmu-miR-383	MIMAT0000748	–
mmu-miR-384	MIMAT0001076	–
mmu-miR-409	MIMAT0001090	–
mmu-miR-410	MIMAT0001091	–
mmu-miR-412	MIMAT0001094	–
mmu-miR-425	MIMAT0001342	–
mmu-let-7a	MIMAT0000521	let-7
mmu-let-7b	MIMAT0000522	let-7
mmu-let-7c	MIMAT0000523	let-7
mmu-let-7d	MIMAT0000383	let-7
mmu-let-7e	MIMAT0000524	let-7
mmu-let-7f	MIMAT0000525	let-7
mmu-let-7g	MIMAT0000121	let-7
mmu-let-7i	MIMAT0000122	let-7
mmu-miR-15a	MIMAT0000526	miR-15
mmu-miR-15b	MIMAT0000124	miR-15
mmu-miR-16	MIMAT0000527	miR-16
mmu-miR-195	MIMAT0000225	miR-16
mmu-miR-19a	MIMAT0000651	miR-19
mmu-miR-19b	MIMAT0000513	miR-19

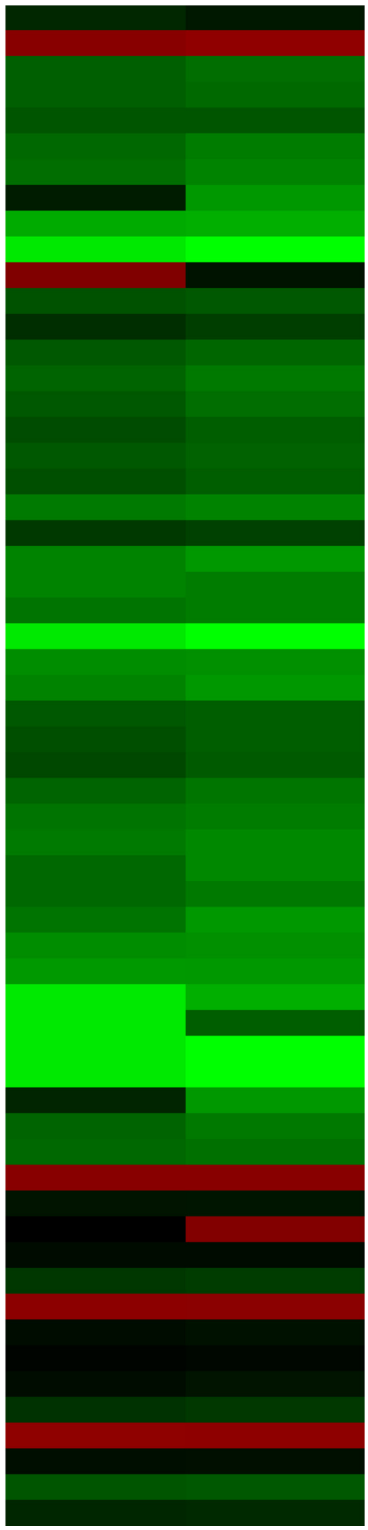

Fig. S1. Continued.

mmu-miR-20	MIMAT0000529	miR-20
mmu-miR-93	MIMAT0000540	miR-20
mmu-miR-106a	MIMAT0000385	miR-20
mmu-miR-106b	MIMAT0000386	miR-20
mmu-miR-23a	MIMAT0000532	miR-23
mmu-miR-23b	MIMAT0000125	miR-23
mmu-miR-25	MIMAT0000652	miR-25
mmu-miR-92	MIMAT0000539	miR-25
mmu-miR-26a	MIMAT0000533	miR-26
mmu-miR-26b	MIMAT0000534	miR-26
mmu-miR-27a	MIMAT0000537	miR-27
mmu-miR-27b	MIMAT0000126	miR-27
mmu-miR-29a	MIMAT0000535	miR-29
mmu-miR-29b	MIMAT0000127	miR-29
mmu-miR-29c	MIMAT0000536	miR-29
mmu-miR-30a-5p	MIMAT0000128	miR-30
mmu-miR-30b	MIMAT0000130	miR-30
mmu-miR-30c	MIMAT0000514	miR-30
mmu-miR-30d	MIMAT0000515	miR-30
mmu-miR-30e	MIMAT0000248	miR-30
mmu-miR-34a	MIMAT0000542	miR-34
mmu-miR-34b	MIMAT0000382	miR-34
mmu-miR-34c	MIMAT0000381	miR-34
mmu-miR-99a	MIMAT0000131	miR-99
mmu-miR-99b	MIMAT0000132	miR-99
mmu-miR-101a	MIMAT0000133	miR-101
mmu-miR-101b	MIMAT0000616	miR-101
mmu-miR-125a	MIMAT0000135	miR-125
mmu-miR-125b	MIMAT0000136	miR-125
mmu-miR-130a	MIMAT0000141	miR-130
mmu-miR-130b	MIMAT0000387	miR-130
mmu-miR-141	MIMAT0000153	miR-141
mmu-miR-200a	MIMAT0000519	miR-141
mmu-miR-200b	MIMAT0000233	miR-141
mmu-miR-200c	MIMAT0000657	miR-141
mmu-miR-181a	MIMAT0000210	miR-181
mmu-miR-181b	MIMAT0000673	miR-181
mmu-miR-290	MIMAT0000366	miR-290
mmu-miR-292-5p	MIMAT0000369	miR-290
mmu-miR-291-3p	MIMAT0000368	miR-291
mmu-miR-294	MIMAT0000372	miR-291
mmu-miR-300	MIMAT0000378	miR-300
mmu-miR-381	MIMAT0000746	miR-300
mmu-let-7d*	MIMAT0000384	-
mmu-miR-9*	MIMAT0000143	-
mmu-miR-189	MIMAT0000218	-
mmu-miR-30e*	MIMAT0000249	miR-30a-3p
mmu-miR-126-5p	MIMAT0000137	-
mmu-miR-129-3p	MIMAT0000544	-
mmu-miR-140*	MIMAT0000152	-
mmu-miR-199a*	MIMAT0000230	-
mmu-miR-424	MIMAT0000548	-
mmu-miR-411	MIMAT0001093	-
mmu-miR-431	MIMAT0001418	-
mmu-miR-433-3p	MIMAT0001420	-
mmu-miR-433-5p	MIMAT0001419	-
mmu-miR-434-3p	MIMAT0001422	-
mmu-miR-434-5p	MIMAT0001421	-
mmu-miR-463	MIMAT0002104	-

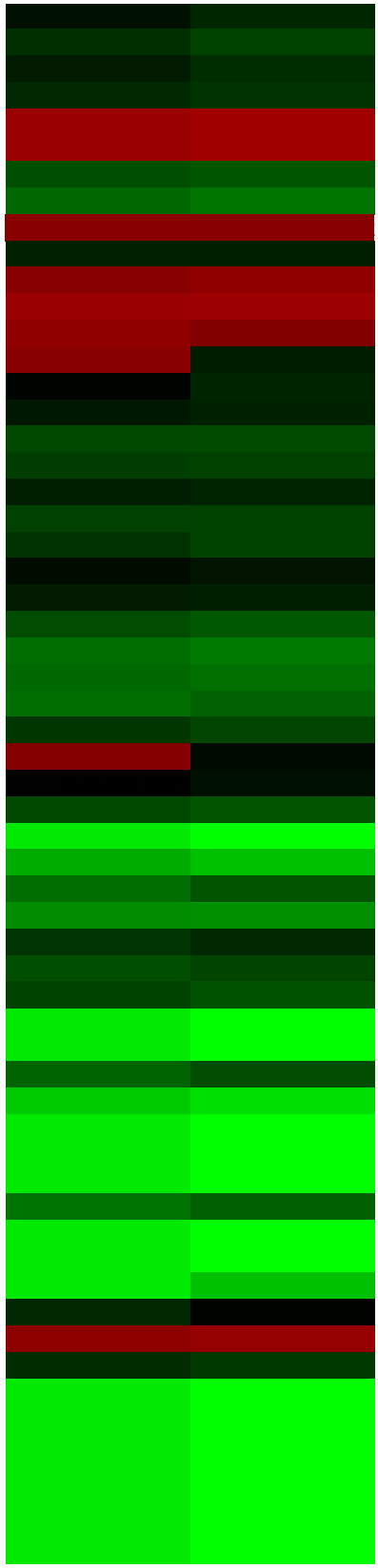

Fig. S1. Continued.

mmu-miR-464	MIMAT0002105	-
mmu-miR-465	MIMAT0002106	-
mmu-miR-466	MIMAT0002107	-
mmu-miR-467	MIMAT0002108	-
mmu-miR-468	MIMAT0002109	-
mmu-miR-469	MIMAT0002110	-
mmu-miR-470	MIMAT0002111	-
mmu-miR-471	MIMAT0002112	-
Cont 1	-	-
Cont 2	-	-
Cont 4	-	-
Cont 5	-	-
Cont 6	-	-
Cont 7	-	-
Cont 8	-	-
Cont 9	-	-
Cont 10	-	-
mmu-mir-321	MI0000705	-

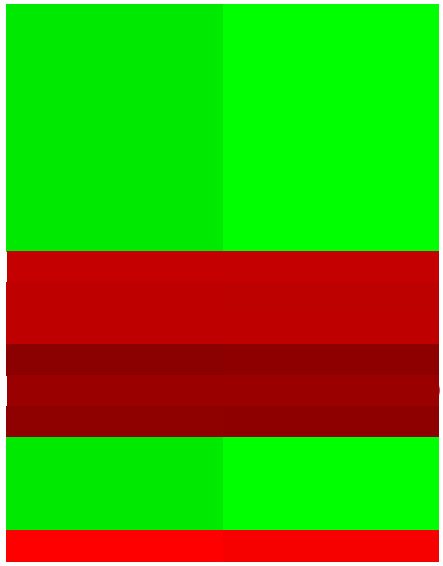

Fig. S1. Continued.

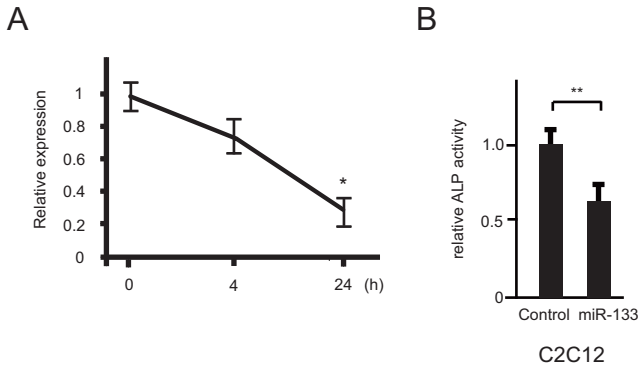

Fig. S2. Regulation of osteoblast differentiation by miR-133. (*A*) Change in miR-133 expression during osteoblast differentiation: Primary osteoblasts were treated in differentiation medium with BMP-2 for each indicated length of time. Quantitative RT-PCR analysis. Note the significant decrease in parallel with the progression of osteoblast differentiation. *, $P < 0.05$ vs. 0 time point, $n = 6$. (*B*) Effect of miR-133 expression on BMP-2-dependent C2C12 cell differentiation: C2C12 cells constitutively expressing miR-133 were cultured in a differentiation medium containing BMP-2. Alkaline phosphatase activity was analyzed. Note the decreased osteoblastic differentiation. *, $P < 0.05$, $n = 6$.

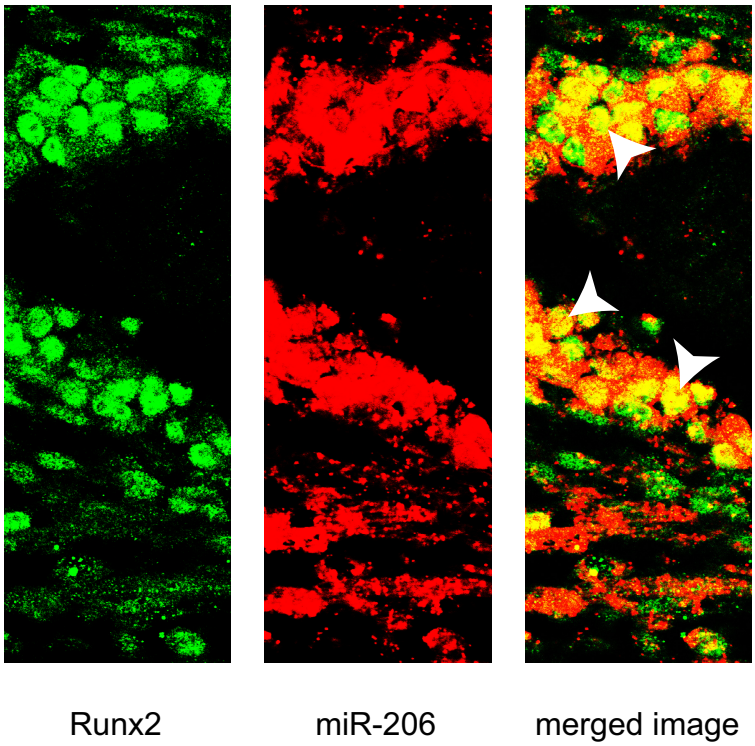

Fig. S3. Colocalization of miR-206 with Runx2 in osteoblasts. Double staining analysis for in situ hybridization to detect miR-206 and immunohistochemistry to detect Runx2 in mouse embryos: Rib (E14.5) cryosections. Runx2 localization (*Left*, green), miR-206 localization (*Middle*, red), and merged image of green and red fluorescence (*Right*, yellow). Note the co-localization of miR-206 and Runx2 expression in perichondrium (arrowheads). Images were taken using confocal microscope. Image magnification, ×40.

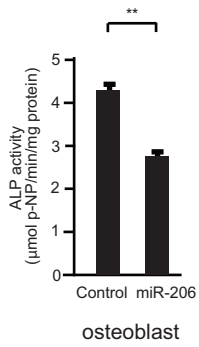

Fig. S4. Regulation of BMP-2-dependent osteoblast differentiation by miR-206. Effect of miR-206 continuous expression on primary osteoblast differentiation: primary mouse osteoblasts infected with pAd-miR-206 or control adenovirus were cultured in the presence of BMP-2. Alkaline phosphatase activity assay was analyzed. Note the decreased osteoblastic differentiation in miR-206 expressing cells. **, $P < 0.01$, $n = 6$.

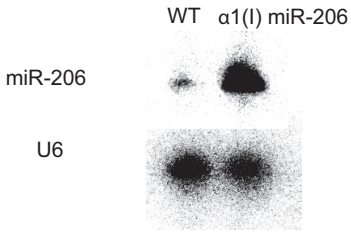

Fig. S5. miR-206 transgene expression was confirmed by Northern blot in α1(I) miR-206 tg mice. Total RNA was isolated from mouse femur. Note the distinct miR-206 expression in α1(I) miR-206 tg mice.